

## Kinetics of conformational changes associated with potassium binding to and release from $\text{Na}^+/\text{K}^+$ -ATPase

Promod R. Pratap<sup>a,\*</sup>, Anuradha Palit<sup>a</sup>, Eva Grassi-Nemeth<sup>b</sup>, Joseph D. Robinson<sup>b</sup>

<sup>a</sup> Department of Physics and Astronomy, University of North Carolina at Greensboro, 101 Petty Science Bldg., Greensboro, NC 27412-5001, USA

<sup>b</sup> Department of Pharmacology, SUNY Health Science Center, Syracuse, NY 13210, USA

Received 16 April 1996; revised 20 June 1996; accepted 20 June 1996

### Abstract

The  $\text{Na}^+/\text{K}^+$ -ATPase functions in cells to couple energy from the hydrolysis of ATP to the transport  $\text{Na}^+$  out and  $\text{K}^+$  in. The fluorescent probe IAF (iodoacetamidofluorescein) covalently binds to this enzyme, reporting conformational changes without inhibiting enzyme activity. This paper describes experiments using dog kidney enzyme labeled with IAF to examine kinetics of conformational changes resulting from added  $\text{Na}^+$  and  $\text{K}^+$ , measured in terms of steady-state and stopped-flow fluorescence changes. Kinetics of these fluorescence changes were examined as a function of temperature from two initial conditions: (a) enzyme in the high-fluorescence form ( $E_{\text{high}}$ ) was rapidly mixed with varying  $[\text{K}^+]$ ; and (b) enzyme in the low-fluorescence form ( $E_{\text{low}}$ ) was rapidly mixed with varying  $[\text{ATP}]$ . These experiments showed: (1) The rate constant for the fluorescence change from  $E_{\text{high}}$  to  $E_{\text{low}}$  was much larger than that for the opposite transition,  $E_{\text{low}}$  to  $E_{\text{high}}$ ; (2) the apparent free energy of activation ( $E_a^{\text{app}}$ ) for the two transitions were different (as estimated from Arrhenius plots); (3) under steady-state conditions, IAF fluorescence did not change when ATP was added to  $E_{\text{low}}$  ( $\text{K}^+$ ) in the absence of  $\text{Na}^+$ ; (4) the apparent free energy of activation was independent of  $[\text{K}^+]$  for the  $E_{\text{high}}$  to  $E_{\text{low}}$  transition (at 16.4 kcal/mol) but increased with  $[\text{ATP}]$  for the  $E_{\text{low}}$  to  $E_{\text{high}}$  transition; (5)  $E_a^{\text{app}}$  for the  $E_{\text{low}}$  to  $E_{\text{high}}$  transition with 1 mM ATP was approximately the same as that in the absence of ATP (34 kcal/mol). These results can be interpreted as: (i) in the transition from  $E_{\text{low}}$  to  $E_{\text{high}}$ , IAF reported a conformational change that occurred after  $\text{K}^+$  release to the intracellular side and which is involved in  $\text{Na}^+$  binding; (ii)  $E_a^{\text{app}}$  increased with  $[\text{ATP}]$ , while increasing the entropy of the transition state. Thus, ATP appeared to destabilize the enzyme during the transition from  $E_{\text{low}}$  to  $E_{\text{high}}$ .

**Keywords:** ATPase,  $\text{Na}^+/\text{K}^+$ ; Reaction sequence; Kinetics; Conformational change; Ion transport

Abbreviations: AMP-PNP, 5'-adenylylimidodiphosphate; BIPM, *N*-(2-benzimidazolyl)phenylmaleimide;  $E_{\text{high}}$  and  $E_{\text{low}}$ , high- and low-fluorescence forms of  $\text{Na}^+/\text{K}^+$ -ATPase labeled with IAF;  $E_{\text{low}}(\text{K}^+)$ ,  $E_{\text{low}}$  form of the enzyme with  $\text{K}^+$  occluded;  $E_{\text{high}}\text{P}$  and  $E_{\text{low}}\text{P}$ , phosphorylated forms of  $E_{\text{high}}$  and  $E_{\text{low}}$ ;  $E_1$ ,  $E_2$ , conformations of the  $\text{Na}^+/\text{K}^+$ -ATPase according to the Albers-Post cycle;  $E_1\text{P}$ ,  $E_2\text{P}$ , phosphorylated forms of  $E_1$ ,  $E_2$ ;  $E^*\text{P}$ , proposed intermediate phosphoenzyme;  $E_a^{\text{app}}$ , apparent free energy of activation; IAF, 5-iodoacetamidofluorescein;  $\text{Na}^+/\text{K}^+$ -ATPase, sodium plus potassium-dependent adenosine triphosphatase (EC 3.6.1.3); RH421, *N*-(4-sulfobutyl)-4-(4-(*p*-dipentylaminophenyl)butadienyl)pyridinium.

\* Corresponding author. Fax: +1 (910) 334-5865; e-mail: pratapp@dirac.unc.edu.

## 1. Introduction

According to the Albers–Post model of  $\text{Na}^+/\text{K}^+$ -ATPase function (Fig. 1), the enzyme exists in two conformations,  $E_1$  and  $E_2$ , each of which can be either phosphorylated or not [1]. The  $E_1$  conformation is often depicted as (a) having cation binding sites that face the cytoplasmic medium in situ; (b) binding  $\text{Na}^+$  with higher affinity than other monovalent cations; and (c) binding ATP with high affinity. Conversely, the  $E_2$  conformation is depicted as (a) having cation binding sites that face the extracellular medium; (b) binding  $\text{K}^+$  and  $\text{Rb}^+$  with higher affinity than  $\text{Na}^+$ ; and (c) binding ATP with an affinity two to three orders of magnitude lower than  $E_1$ . In accord with the scheme, the two conformations exhibited different trypsin digestion patterns and different fluorescence quantum efficiencies for various fluorescent probes. Sodium transport across the membrane was associated with the conformational transitions from  $E_1\text{P}$  to  $E_2\text{P}$ , and potassium transport with transitions from  $E_2$  to  $E_1$ .

This Albers–Post scheme in its further developments [2] adequately explained steady-state experiments but was less successful in accommodating transient kinetic data. For example, in order to explain their data, Yoda and Yoda [3–6] had to postulate a third phosphoenzyme,  $E^*\text{P}$  specified as binding two  $\text{Na}^+$  (the third  $\text{Na}^+$  having been released to the extracellular side) and sensitive to dephosphorylation by ADP.

A fundamental question therefore is: what exactly

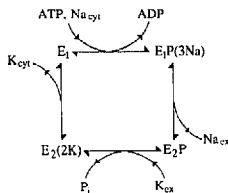


Fig. 1. Albers–Post mechanism of the  $\text{Na}^+/\text{K}^+$ -ATPase.  $E_1$  is the  $\text{Na}^+$ -sensitive form (corresponds to  $E_{\text{high}}$  under steady-state conditions);  $E_2$  is the  $\text{K}^+$ -sensitive form (corresponds to  $E_{\text{low}}$  under steady-state conditions).

is meant by the  $E_1$  to  $E_2$  conformational change? Does there exist a well-defined step at which all properties of the  $E_1$  conformation switch to those of the  $E_2$  conformation, or does the definition of  $E_1$  and  $E_2$  depend upon the techniques used to measure the conformational change? Comparisons [7–9] between the transient kinetics of conformational change (as reported by fluorescence changes of IAF- and BIPM-labeled enzyme) and charge transport (as reported by the electrochromic dye RH421) indicated that (a) IAF reported a transition that occurs after the release of at least one  $\text{Na}^+$  to the extracellular side; (b) BIPM reported the release of the first  $\text{Na}^+$ ; and (c) RH421 reported the release of the second and/or third  $\text{Na}^+$  to the extracellular side. Those results suggested that a simple Albers–Post scheme is inadequate for interpreting transient kinetics of the ATPase.

Because of these uncertainties, results in this paper are interpreted operationally in terms of the measured high- and low-fluorescence states of the labeled enzyme ( $E_{\text{high}}$  and  $E_{\text{low}}$ ). Under steady-state conditions in the absence of enzyme cycling,  $E_{\text{high}}$  and  $E_{\text{low}}$  correspond to  $E_1$  and  $E_2$ , respectively. This equivalence, however, breaks down under transient-state conditions.

Both steady-state and transient kinetics of  $\text{K}^+$  transport and correlated conformational states have been examined earlier using radioactive ligands such as  $^{86}\text{Rb}$  and  $^{42}\text{K}$  and fluorescent probes such as FITC, eosin and IAF [2,10–16]. Recently, Hasenauer et al. [17] examined the kinetics of  $^{86}\text{Rb}$  deocclusion from dog kidney enzyme and found that ATP in the absence of  $\text{Na}^+$  causes deocclusion but not release of  $^{86}\text{Rb}$  from the enzyme, whereas  $\text{Na}^+$  and choline lowered the affinity of the cation binding site to  $\text{Rb}^+$ . These results are consistent with the earlier results by Shani et al. [18].

This paper reports results of experiments using IAF-labeled enzyme to address three questions: (a) What are the rate-limiting steps in the 'forward' and 'backward' directions (defined with reference to the direction of the enzyme reaction cycle in vivo) and what are their kinetic properties? (b) Where along the reaction sequence does IAF fluorescence change? and (c) What are the effects of ATP and  $\text{Na}^+$  on the  $E_{\text{low}}$  ( $\text{K}^+$ ) form ( $E_{\text{low}}$  with occluded  $\text{K}^+$ ) of the enzyme?

## 2. Materials and methods

Frozen dog kidneys were obtained from Pel-Freez Biologicals (Rogers, AR), and IAF from Molecular Probes (Eugene, OR). Low-fluorescence imidazole, EDTA and ATP were from Sigma (St. Louis, MO); reagent-grade salts were either from Sigma or from Mallinckrodt (Paris, KY).

$\text{Na}^+/\text{K}^+$ -ATPase was isolated from the outer medulla of the kidney by a modification of method C of Jørgensen [19]; specific activity was in the range of 10–25  $\mu\text{mol P}_i$  (mg protein) $^{-1}$  min $^{-1}$  at 37°C. Enzyme was labeled with IAF as described earlier [7].

Steady-state experiments were performed as described before [7,8] using a Perkin-Elmer fluorescence spectrophotometer (model MPF-66; Perkin-Elmer, Oak Brook, IL). Stopped-flow experiments were performed using a stopped-flow fluorimeter (Kinetic Instruments, Ann Arbor, MI) interfaced with a Macintosh IIcx personal computer (Apple Computer, Cupertino, CA) through a MacADIOS interface board (GW Instruments, Somerville, MA), as described earlier [7,8]. For IAF-enzyme, fluorescence excitation wavelength ( $\lambda_{\text{ex}}$ ) was 492 nm; emission was measured with a photomultiplier tube using a cutoff filter (Corning 3-69) with the wavelength of 50% transmission ( $\lambda_{1/2}$ ) = 529 nm. The fluorimeter was connected to a refrigerated circulating water bath; the syringes, mixer, and observation chamber were immersed in water from the water bath.

## 3. Results

### 3.1. Transition from $E_{\text{high}}$ to $E_{\text{low}}$

Fig. 2 shows a typical fluorescence trace when IAF-enzyme plus  $\text{Na}^+$  was mixed rapidly with 5 mM  $\text{K}^+$ . Over the time scale shown in the figure, this fluorescence change was fitted by a single exponential with an observed rate constant ( $k_{\text{obs}}$ ) of 81 s $^{-1}$ .

The rate constant of the fluorescence change ( $k_{\text{obs}}$ ) was measured as a function of  $[\text{K}^+]$  at three different temperatures (15, 20 and 25°C; Fig. 3). These data were fitted with a Hill equation, yielding  $k_{\text{obs}}^{\text{max}}$ ,  $K_{1/2}$  and Hill coefficient  $n$  at each temperature. Only  $k_{\text{obs}}^{\text{max}}$

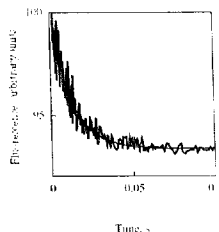


Fig. 2. Typical traces of IAF fluorescence change for  $E_{\text{high}} \rightarrow E_{\text{low}}$  transition. IAF-enzyme (100  $\mu\text{g}/\text{ml}$  in buffer with 150 mM choline chloride, 3.1 mM NaCl, 1 mM EDTA, 25 mM imidazole-HCl, pH 7) was rapidly mixed with 5 mM  $\text{KCl}$  (2.5 mM final concentration after mixing) in the same buffer (choline chloride concentration was adjusted to maintain ionic strength) at 20°C. In this and other figures, fluorescence was at 100% at time zero. The trace was fitted reasonably well to a single exponential with the fluorescence rate constant  $k_{\text{obs}} = 81 \text{ s}^{-1}$ .

varied with temperature;  $K_{1/2}$  was about 2.5 mM and  $n$  was about 1.5 at all three temperatures.

An apparent energy of activation  $E_a^{\text{app}}$  was determined from Arrhenius plots (Fig. 4A) and plotted against  $[\text{K}^+]$  (Fig. 4B).  $E_a^{\text{app}}$  had an average value of 16.4 kcal/mol, and did not vary significantly with  $[\text{K}^+]$  over the range of concentration studied.

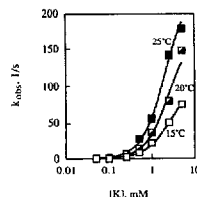


Fig. 3.  $k_{\text{obs}}$  for the  $E_{\text{high}} \rightarrow E_{\text{low}}$  transition at 15, 20 and 25°C, vs.  $[\text{K}^+]$  (final concentration after mixing). Lines represent fits to the Hill equation, with  $K_{1/2} = 2.5 \pm 0.5 \text{ mM}$  and the Hill coefficient  $n_H = 1.5$  at all three temperatures, and  $k_{\text{obs}}^{\text{max}} = 108 \pm 17 \text{ s}^{-1}$  (15°C),  $174 \pm 27 \text{ s}^{-1}$  (20°C), and  $239 \pm 32 \text{ s}^{-1}$  (25°C) (mean  $\pm$  S.E.M.). Experimental conditions were as in Fig. 2.

### 3.2. Transition from $E_{low}$ to $E_{high}$

Fig. 5 shows the steady-state fluorescence change when increasing amounts of ATP were added to enzyme in  $E_{low}(K^+)$  form ( $E_{low}$  with occluded  $K^+$ ) in the presence and absence of 0.1 mM  $Na^+$ . In the absence of  $Na^+$ , no significant fluorescence changes were observed except at 5 mM ATP. In the presence of  $Na^+$ , fluorescence increased, with  $K_{1/2}$  greater than 200  $\mu$ M ATP. This estimate is much higher than the  $K_m$  for enzyme phosphorylation and is consistent with reported values for ATP accelerating  $K^+$  deocclusion.

Fig. 6 shows typical fluorescence traces when

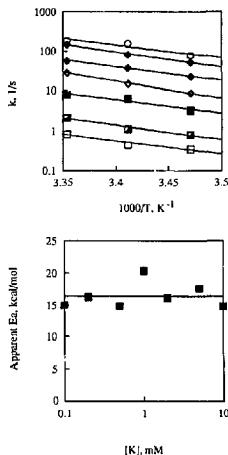


Fig. 4. (A, top) Arrhenius plot of observed rate constant  $k$  for fluorescence change associated with the  $E_{high} \rightarrow E_{low}$  transition at various  $[K^+]$  ( $\log(k)$  vs.  $1/(\text{absolute temperature})$ ). 100  $\mu$ g/ml enzyme in buffer (150 mM choline chloride, 1 mM NaCl, 1 mM EDTA, 25 mM imidazole-HCl, pH 7) was rapidly mixed with varying concentrations of  $K^+$  in the same buffer. Symbols represent different  $[K^+]$  ( $\square = 0.1$  mM;  $\blacksquare = 0.2$  mM;  $\bullet = 0.5$  mM;  $\diamond = 2$  mM;  $\circ = 10$  mM). (B, bottom)  $E_a^{app}$ , evaluated from the slopes of the straight lines in (A).

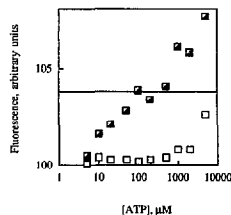


Fig. 5. Steady-state fluorescence changes from  $E_{low}$  to  $E_{high}$  in the presence ( $\blacksquare$ ) and absence ( $\square$ ) of 0.1 mM  $Na^+$ . IAF-enzyme (15  $\mu$ g/ml) was suspended in buffer (25 mM imidazole-HCl, pH 7, 1 mM EDTA, 0.1 mM NaCl, 150 mM choline chloride, 5 mM KCl). [ATP] was increased by serial additions. Observed fluorescence was noted and corrected for dilution.

IAF-enzyme plus 5 mM  $K^+$  ( $E_{low}(K^+)$ ) plus 50 mM choline chloride was rapidly mixed with ATP plus 55 mM  $Na^+$  (sufficient to saturate the  $Na^+$  binding sites) at 20°C (final  $[A^+P] = 0, 0.5$  and 1 mM). ATP increased the rate constant of fluorescence change. These increases are consistent with reported values for acceleration of deocclusion by ATP.

These rates were examined as a function of the

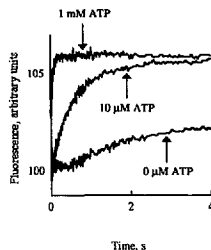


Fig. 6. Typical traces of IAF fluorescence change for  $E_{low} \rightarrow E_{high}$  transition. IAF-enzyme (100  $\mu$ g/ml) in buffer with 50 mM choline chloride, 5 mM KCl, 1 mM EDTA, 25 mM imidazole-HCl (pH 7), was mixed rapidly at 20°C with ATP in buffer with 55 mM NaCl, 1 mM EDTA, 25 mM imidazole-HCl (pH 7). ATP concentrations indicated on the plots are those immediately after mixing. Observed fluorescence rate constants were:  $31 \text{ s}^{-1}$  (1 mM ATP),  $1.9 \text{ s}^{-1}$  (10  $\mu$ M ATP), and  $0.45 \text{ s}^{-1}$  (0 ATP).

reaction temperature at various [ATP]. At all temperatures,  $k_{\text{obs}}$  increased with [ATP]; when [ATP] was increased from 0 to 1 mM, the rate constant increased 12- to 60-fold. The data were fitted to the Hill equation (not shown); although those plots were not well defined (because of scatter in the points), they

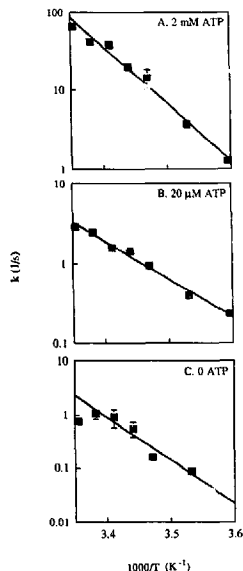


Fig. 7. (A, B) Arrhenius plots of observed  $k_{\text{obs}}$  for the  $E_{\text{obs}} \rightarrow E_{\text{high}}$  transition induced by 1 mM and 10  $\mu\text{M}$  ATP. 100  $\mu\text{g}/\text{ml}$  enzyme in buffer (50 mM choline chloride, 25 mM imidazole-HCl, 1 mM EDTA) was rapidly mixed with ATP (final concentrations: 10  $\mu\text{M}$  or 1 mM). The solid lines are fits of the Arrhenius equation to the data, with  $E_a^{\text{app}} = 33$  kcal/mol (1 mM) and 22 kcal/mol (10  $\mu\text{M}$ ). (C) Arrhenius plot for  $E_{\text{low}} \rightarrow E_{\text{high}}$  transition at 0 ATP. Other conditions same as in parts A and B. The line is a fit to all the data except the 25°C point, with  $E_a^{\text{app}} = 37$  kcal/mol. If the 25°C point was included,  $E_a^{\text{app}} = 29$  kcal/mol.

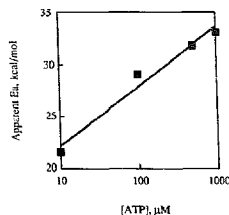


Fig. 8.  $E_a^{\text{app}}$  for the ATP-induced fluorescence change plotted against  $\log[\text{ATP}]$ . The solid line is a straight line fit to this plot, with slope = 5.8 kcal/mol, and intercept (at 1  $\mu\text{M}$  ATP) = 16 kcal/mol.

suggested a Hill coefficient of 1 at all temperatures, consistent with a single binding site.

Arrhenius plots of  $k_{\text{obs}}$  against the absolute temperature were used to quantify the temperature dependence of the rate constant (Fig. 7). In the presence of ATP (10  $\mu\text{M}$  and 1 mM Fig. 7A and B), these plots were fitted well by a straight line ( $r^2 > 0.94$ ). In the absence of ATP,  $\log(k_{\text{obs}})$  was nonlinear with  $1/T$ . As the temperature was increased from 20 to 25°C,  $k_{\text{obs}}$  decreased significantly. Although this decrease was seen at only one temperature, it was reproducible over three experiments.

Plots of apparent free energy of activation ( $E_a^{\text{app}}$ ) against [ATP] (Fig. 8) indicated that  $E_a^{\text{app}}$  increased with increasing [ATP], from 21 to 33 kcal/mol.  $E_a^{\text{app}}$  at 10  $\mu\text{M}$  was about 22 kcal/mol, while  $E_a^{\text{app}}$  at 1  $\mu\text{M}$  was estimated by extrapolation to be 16 kcal/mol. These concentrations of ATP were two or three orders of magnitude lower than that required to induce  $\text{K}^+$  deocclusion [16]; by contrast, the Arrhenius plot at 0 ATP (without the point at 25°C) yielded a much higher  $E_a^{\text{app}}$  of 37 kcal/mol. (Even if the point at 25°C were included, the calculated  $E_a^{\text{app}}$  was 29 kcal/mol.)

### 3.3. Effects of $\text{Mg}^{2+}$

In order to prevent enzyme phosphorylation and ATP hydrolysis, the experiments reported here were performed in the absence of  $\text{Mg}^{2+}$ . In order to exam-

Table 1

Effect of  $Mg^{2+}$  on transient kinetics of  $E_{low} \rightarrow E_{high}$  transition

Experimental conditions	Magnitude (% $\Delta F$ )	Rate constant ( $s^{-1}$ )
– Nucleotide	$2.4 \pm 0.4$	$6.0 \pm 0.3$
0.5 mM ATP, – $Mg^{2+}$	$4.4 \pm 0.9$	$46 \pm 5$
0.5 mM AMP-PNP	$4.6 \pm 0.8$	$13.3 \pm 3.2$
0.5 mM AMP-PNP + 4 mM $Mg^{2+}$	$6.0 \pm 0.3$	$6.2 \pm 1.1$

100  $\mu g/ml$  enzyme in 25 mM imidazole-HCl (pH 7.0), 1 mM EDTA,  $\pm 4$  mM  $MgCl_2$ , 155 mM choline chloride, 5 mM KCl, was rapidly mixed with 1 mM nucleotide (ATP or AMP-PNP; final concentration 0.5 mM) in 25 mM imidazole-HCl (pH 7.0), 1 mM EDTA, 30 mM choline chloride, 110 mM NaCl, in the presence of absence of 4 mM  $MgCl_2$ , in both syringes. Results in the absence of nucleotide are also shown for comparison. Magnitude and rate constants are expressed as the mean of three experiments  $\pm$  standard error of the mean. Nucleotide concentrations listed are the final concentrations, after mixing.

ine the effects of this omission, the rate constant for the  $E_{low} \rightarrow E_{high}$  fluorescence change was measured in the presence of  $Mg^{2+}$  but with AMP-PNP instead of ATP. Table 1 lists these rate constants.

#### 4. Discussion

Under steady-state conditions, fluorescence intensities of IAF-labeled enzyme could be correlated with  $E_1$  and  $E_2$  conformations of standard models [20]. Earlier, the sodium-transporting part of the enzyme reaction cycle were examined under non-steady-state conditions with IAF-enzyme [7,11]. Under those conditions, however, IAF fluorescence changes corresponded to steps in the reaction cycle that followed the release of the first  $Na^+$  to the extracellular side of the enzyme. On that basis, standard models – in which the conformational changes are tightly coupled to all cation transport – do not agree with transient kinetic data. Since the identification is problematic under these transient-state kinetic studies, the two conformation of IAF-labeled enzyme are designated as  $E_{high}$  and  $E_{low}$  in this paper, corresponding to their fluorescence intensities.

Using IAF-enzyme, the kinetics of the  $K^+$ -transporting leg of the enzyme reaction cycle were measured under various conditions for both the 'forward' ( $E_{low} \rightarrow E_{high}$ ) and 'backward' ( $E_{high} \rightarrow E_{low}$ ) transitions. The following questions were addressed:

(a) What are the kinetic properties of the rate-limiting steps (as indicated by IAF fluorescence change) in the 'forward' and 'backward' transitions? In earlier work, Steinberg and Karlsh [16] observed a difference in the rate constant of fluorescence change in the two directions. Although these results were not interpreted, they are consistent with different rate-limiting steps in the two directions.

(b) Where along the reaction cycle does the IAF fluorescence change? For the  $Na^+$ -transporting portion of the reaction cycle, earlier work from this [7,8] and other [11] laboratories have indicated that IAF fluorescence changes after the release of at least the first  $Na^+$  at the extracellular face of the protein. Thus, IAF fluorescence reflects changes that occur after the traditional  $E_1P$  to  $F_2P$  transition.

(c) What are the effects of ATP,  $Na^+$  and choline on the 'forward' transition ( $E_{low} \rightarrow E_{high}$ ) of the enzyme?

In analyzing data presented here, the following assumption were made: (a) IAF fluorescence changes at a single step and that this step is the same in the 'forward' and 'backward' transitions; in other words, the 'backward' reaction was assumed to go through the same steps as the 'forward' reaction, but in reverse order; and (b) there were no branches in the reaction schemes for each of the two sets of conditions in the 'forward' direction (presence or absence of ATP).

A further assumption was that ATP induces both  $K^+$  deocclusion and release. Recently, Hasenauer et al. [17] reported that ATP, in the absence of  $Na^+$  and at low ionic strength, increased the rate constants for both  $Rh^+$  binding and release without, however, affecting its affinity. On the other hand, higher concentrations of  $Na^+$  and choline – such as those used here – promote  $K^+$  deocclusion. Then, since IAF fluorescence did not change in the absence of  $Na^+$  (but the presence of choline chloride) under steady-state conditions (Fig. 5), and since ATP in the absence of  $Na^+$  (and presence of choline chloride) induces  $K^+$ -deocclusion and release, IAF fluorescence must change at some step associated with  $Na^+$  binding to the enzyme.

This conclusion is supported by the differences in the fluorescence rate constant ( $k_{obs}$ ) and its temperature dependence (and apparent free energy of activation  $E_a^{app}$ ). These observations imply that IAF reports

different rate-limiting steps for the two transitions. (Differences in  $k_{obs}$  have been reported earlier [16].)

Since these experiments use fluorescence as a kinetic probe, the end point of a sequence of steps is, by definition, the step at which the fluorescence changes; subsequent steps are fluorescently silent. Therefore, results reported here are consistent with the end point of the sequence of steps in the 'forward' direction not being the starting point of the sequence of steps in the 'backward' direction.

The Arrhenius plots for the two transitions yielded an apparent activation energy ( $E_a^{app}$ ) each.  $E_a^{app}$  was independent of  $[K^+]$  for the 'backward' reaction. However, for the 'forward' reaction,  $E_a^{app}$  increased with  $[ATP]$ , by a factor of 2 over the range of ATP concentrations studied. An increase in  $E_a^{app}$  implies a decrease in  $k_{obs}$ , if all other parameters are unchanged in the Arrhenius equation. [21]:

$$\log(k_{obs}) = -\frac{E_a^{app}}{2.3 R T} + \log(A) \quad (1)$$

However, if  $A$  increases with  $[ATP]$ ,  $k_{obs}$  could increase.

$A$  shows the approximate equivalence [22]:

$$A \equiv \kappa \left( \frac{kT}{h} \right) \exp \left( \frac{\Delta S^\ddagger}{R} \right) \quad (2)$$

where  $\kappa$  is the quantum mechanical probability that a system that attains the energy  $E_a^{app}$  will proceed to complete the reaction;  $\Delta S^\ddagger$  is the standard entropy of activation;  $k$  is the Boltzmann constant and  $h$  is the Planck constant. Since  $A$  increases exponentially with  $\Delta S^\ddagger$  in this model,  $k_{obs}$  could increase with  $[ATP]$  if ATP binding induced an increase in  $\Delta S^\ddagger$ .

Since  $\Delta S^\ddagger$  is a measure of the change in entropy when the enzyme goes from  $E_{low}$  to the transition state, this model implies that ATP increases the entropy of the transition state. Physically, this might indicate that although the transition state has higher energy when ATP is bound, this state has a greater degeneracy than in the absence of ATP, so an increase in the transition energy is compensated by an increase in the number of ways the protein can attain that state.

In the absence of ATP,  $E_a^{app}$  was much higher than

in the presence of low (10  $\mu M$ ) ATP (Fig. 7C, Fig. 8). Further,  $E_a^{app}$  increased monotonically with  $[ATP]$  for concentrations greater than 10  $\mu M$ . An upper limit for the affinity of ATP for this decrease in  $E_a^{app}$  can be estimated as follows:

$E_a^{app}$  decreases from 29–37 kcal/mol at 0 ATP to 16.4 kcal/mol at 10  $\mu M$  ATP; it then increases as ATP increases. Because no values for  $E_a^{app}$  were determined for concentrations between 10 and 100  $\mu M$  ATP, it may be argued that  $E_a^{app}$  continued to drop as ATP was increased beyond 10  $\mu M$ , but then increased to its value at 100  $\mu M$  ATP. Even with this interpretation of the data,  $E_a^{app}$  must reach a minimum between 10 and 100  $\mu M$  ATP. Thus, the  $K_{1/2}$  for this effect must be much less than 100  $\mu M$ . When compared with that  $K_{1/2}$  for  $K^+$  deocclusion ( $\approx 0.5$  mM), this is a high-affinity effect of ATP. In other words, the change in  $E_a^{app}$  is a composite of two effects: a high-affinity ATP-induced decrease followed by a low-affinity ATP-induced increase.

A further question needs to be addressed here. Experiments described here were performed in the presence of EDTA and in the absence of added  $Mg^{2+}$ . Magnesium is necessary for enzyme activity because ATP is active as Mg-ATP in vivo and because the enzyme has a binding site for  $Mg^{2+}$  [23]. Could this lack of  $Mg^{2+}$  explain these various effects of ATP described here? Forbush [13] examined the effect of  $Mg^{2+}$  on this transition when ATP and ADP were used to accelerate it. With ATP he found that  $Mg^{2+}$  increased the transition at low concentrations but decreased it at high concentrations. On the other hand, with ADP he found that  $Mg^{2+}$  only decreased the rate. Those experiments were performed in the absence of  $Na^+$ .

Under the experimental condition used here, the  $E_{low} \rightarrow E_{high}$  transition could not be examined in the absence of  $Na^+$ : the IAF fluorescence change could not be observed in the absence of  $Na^+$  (see Fig. 5), and if  $Na^+$  was present with  $Mg^{2+}$  and ATP, the enzyme would be phosphorylated and fluorescence changes attributable to conformational transitions of the phosphoenzyme would decrease the total observable fluorescence change.

To avoid this phosphorylation, the  $E_{low} \rightarrow E_{high}$  transition was induced with AMP-PNP, an ATP analog that is not hydrolyzed by the enzyme. Again, the fluorescence change was fitted with a single exponen-

tial, which yielded an observed rate constant ( $k_{\text{obs}}$ ) and magnitude ( $\% \Delta F$ ; Table 1). Note that  $k_{\text{obs}}$  reflects the sum of the forward and backward rate constants of the rate-limiting step (in this case  $\text{K}^+$  deocclusion). On the other hand,  $\% \Delta F$  reflects the change in the distribution of  $E_{\text{high}}$  and  $E_{\text{low}}$ , and reflects the equilibrium constant of the step at which this transition takes place (which occurs with or following  $\text{Na}^+$  binding to the enzyme).

In the absence of  $\text{Mg}^{2+}$ ,  $k_{\text{obs}}$  was lower (by a factor of 3) when deocclusion was induced with AMP-PNP than with ATP, although the magnitude of fluorescence change remained the same. These results suggest that AMP-PNP does not increase the rate of  $\text{K}^+$  deocclusion from the enzyme as much as ATP, even though the final distribution of  $E_{\text{high}}$  and  $E_{\text{low}}$  remains the same. Since  $E_{\text{high}}$  and  $E_{\text{low}}$  correspond to  $E_1$  and  $E_2$  under steady-state conditions, these results imply that under these conditions, AMP-PNP and ATP are equally effective in inducing  $\text{K}^+$  deocclusion. The reason for this discrepancy is unclear.

In the presence of  $\text{Mg}^{2+}$ ,  $k_{\text{obs}}$  for the fluorescence change induced with AMP-PNP showed a small decrease. However, interpretation of these results is difficult, because it was unclear whether this new effect was due to the  $\text{Mg}^{2+}$  or the AMP-PNP. If this effect was due to the  $\text{Mg}^{2+}$ , it would imply that  $\text{Mg}^{2+}$  decreases one or both of the rate constants associated with the rate-limiting step seen here.

To examine the kinetics of the enzyme reaction in the 'backward' direction, enzyme in the  $E_{\text{high}}$  form was rapidly mixed with varying  $[\text{K}^+]$ . Again, these measurements were performed at different temperatures. For this transition,  $k_{\text{obs}}$  was two or three times higher than for the corresponding 'forward' transition.  $E_a^{\text{APP}}$  for this transition was calculated from Arrhenius plots; these apparent activation energies were not dependent on  $[\text{K}^+]$ .

All these observations indicate that the rate-limiting steps in the two directions are different. Since IAF fluorescence is assumed to change at the same step in both directions, and since the fluorescence changes at some step associated with  $\text{Na}^+$  binding in the 'forward' direction, the rate-limiting step in the 'backward' direction must occur at or before  $\text{Na}^+$  release.

The conclusions are summarized in Fig. 9. (a) The IAF-enzyme exists in a high- and a low-fluorescence

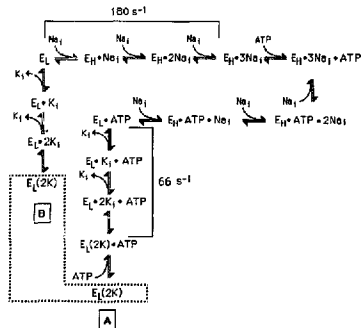


Fig. 9. A proposed reaction scheme for the transport of  $\text{K}^+$  by the  $\text{Na}^+/\text{K}^+ \text{-ATPase}$  in the presence (A) and absence (B) of ATP.  $E_{\text{H}}$  and  $E_{\text{L}}$  correspond to  $E_{\text{high}}$  and  $E_{\text{low}}$  in the text. The conformations of the enzyme included within the dotted lines correspond to the  $E_2$  conformations as proposed in the Albers-Post cycle. The rate-limiting steps and the corresponding rate constants determined (at 25°C) in this paper are shown: for the  $E_{\text{low}} \rightarrow E_{\text{high}}$  transition, the rate constant is from Fig. 7A (1 mM ATP after mixing); for the  $E_{\text{high}} \rightarrow E_{\text{low}}$  transition, the rate constant is from Fig. 3 (5 mM  $\text{K}^+$  after mixing). The numbers were chosen to reflect near-physiological concentrations of ATP and  $\text{K}^+$ .

forms; these forms correspond to the  $E_1$  and  $E_2$  forms of the Albers-Post reaction scheme only under steady-state conditions. (b) The rate-limiting step in the 'forward' direction, as seen by IAF fluorescence change, is  $\text{K}^+$  deocclusion; at high [ATP] (1 mM), the rate constant of fluorescence change (corresponding to  $k_{\text{forward}} + k_{\text{backward}}$  for this step) is  $66 \pm 6 \text{ s}^{-1}$  at 25°C (from Fig. 7A). (c) The rate-limiting step in the 'backward' direction appears to be the displacement of  $\text{Na}^+$  by  $\text{K}^+$ ; at 25°C, the rate constant of the fluorescence change is  $180 \text{ s}^{-1}$  (from Fig. 3). The experiments in this paper indicate that IAF fluorescence changes at the step (or steps) associated with  $\text{Na}^+$  binding to or release from the enzyme. This conclusion is similar to that reached earlier in the study of the  $\text{Na}^+$ -transporting leg of the enzyme cycle [7,8].



## Acknowledgements

Supported by grants from the National Institutes of Health (NS-05430, GM-47550) and the National Science Foundation (DCB-8817355).

## References

- [1] Robinson, J.D. and Fashner, M.S. (1979) *Biochim. Biophys. Acta* 549, 145–179.
- [2] Karlsh, S.J.D. (1980) *J. Bioenerg. Biomembr.* 12, 111–136.
- [3] Yoda, A. and Yoda, S. (1987) *J. Biol. Chem.* 262, 110–115.
- [4] Yoda, S. and Yoda, A. (1986) *J. Biol. Chem.* 261, 1147–1152.
- [5] Yoda, S. and Yoda, A. (1987) *J. Biol. Chem.* 262, 103–109.
- [6] Yoda, A. and Yoda, S. (1988) *J. Biol. Chem.* 263, 10320–10325.
- [7] Pratap, P.R., Robinson, J.D. and Steinberg, M.I. (1991) *Biochim. Biophys. Acta* 1069, 288–298.
- [8] Pratap, P.R. and Robinson, J.D. (1993) *Biochim. Biophys. Acta* 1151, 89–98.
- [9] Bühler, R., Stürmer, W., Apell, H.-J. and Längler, P. (1991) *J. Membr. Biol.* 121, 141–161.
- [10] Stürmer, W., Bühler, R., Apell, H.-J. and Längler, P. (1991) *J. Membr. Biol.* 121, 163–176.
- [11] Heyse, S., Wuddel, I., Apell, H.-J. and Stürmer, W. (1994) *J. Gen. Physiol.* 104, 197–240.
- [12] Smirnova, I.N. and Faller, L.D. (1993) *J. Biol. Chem.* 268, 16120–16123.
- [13] Forbush, B. (1987) *J. Biol. Chem.* 262, 11104–11115.
- [14] Skou, J.C. and Esmann, M. (1983) *Biochim. Biophys. Acta* 746, 101–113.
- [15] Karlsh, S.J.D., Yates, D.W. and Glynn, I.M. (1978) *Biochim. Biophys. Acta* 525, 252–264.
- [16] Steinberg, M. and Karlsh, S.J.D. (1989) *J. Biol. Chem.* 264, 2090–2095.
- [17] Hasenauer, J., Huang, W.-H. and Askari, A. (1993) *J. Biol. Chem.* 268, 3289–3297.
- [18] Shaul, M., Goldschleger, R. and Karlsh, S.J.D. (1987) *Biochim. Biophys. Acta* 904, 13–21.
- [19] Jorgensen, P.L. (1974) *Biochim. Biophys. Acta* 356, 36–52.
- [20] Robinson, J.D. and Pratap, P.R. (1991) *Biochim. Biophys. Acta* 1069, 281–287.
- [21] Segel, I.H. (1975) *Enzyme Kinetics*, John Wiley, New York.
- [22] Johnson, F.H., Eyring, H. and Stover, B.J. (1974) *The Theory of Rate Processes in Biology and Medicine*, John Wiley, New York.
- [23] Robinson, J.D. (1983) *Biochim. Biophys. Acta* 727, 63–69.